AD-A080 561 SOLAR PHYSICS RESEARCH CORP TUCSON AZ F/G 3/2
PHOTOSPHERIC VELOCITY FIELDS AS INDICATORS OF FLARE ACTIVITY.(U)
OCT 79 K L HARVEY, J W HARVEY NOAA-01-8-B01-3883
UNCLASSIFIED AFGL-TR-79-0262 NL

| OF |

AD
A080561

END
3-80

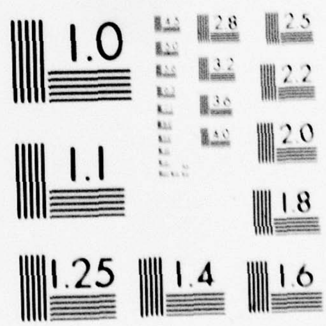

MICROCOPY RESOLUTION TEST CHART
NATIONAL BUREAU OF STANDARDS-1963-A

LEVEL

AFGL-TR-79-0262

AD A080561

# PHOTOSPHERIC VELOCITY FIELDS AS INDICATORS OF FLARE ACTIVITY

K. Harvey
J. Harvey

Solar Physics Research Corporation
4720 Calle Desecada
Tucson, Arizona 85718

314 637

Final Report
11 September - 30 September 1978

October 1979



Approved for public release; distribution unlimited



AIR FORCE GEOPHYSICS LABORATORY
AIR FORCE SYSTEMS COMMAND
UNITED STATES AIR FORCE
HANSCOM AFB, MASSACHUSETTS 01731

80 2 6 003

Qualified requestors may obtain additional copies from the Defense Documentation Center. All others should apply to the National Technical Information Service.

Unclassified

SECURITY CLASSIFICATION OF THIS PAGE (When Data Entered)

19 **REPORT DOCUMENTATION PAGE**

READ INSTRUCTIONS BEFORE COMPLETING FORM

1. REPORT NUMBER

18 AFGL-TR-79-0262

2. GOVT ACCESSION NO.

3. RECIPIENT'S CATALOG NUMBER

4. TITLE (and Subtitle)

6 Photospheric Velocity Fields as Indicators of Flare Activity.

5. TYPE OF REPORT & PERIOD COVERED

Scientific - Final
11 Sept - 30 Sept 1978

6. PERFORMING ORG. REPORT NUMBER

7. AUTHOR(s)

10 K. Harvey [redacted] J. Harvey

8. CONTRACT OR GRANT NUMBER(s)

Project Order ESD 8-0927 to National Oceanic and Atmospheric Administration

9. PERFORMING ORGANIZATION NAME AND ADDRESS

Solar Physics Research Corporation
4720 Calle Desecada
Tucson, Arizona 85718

10. PROGRAM ELEMENT, PROJECT, TASK AREA & WORK UNIT NUMBERS

61102F Task 2311G1
16 ~~WU~~ 2311G101 17 G1

11. CONTROLLING OFFICE NAME AND ADDRESS

Air Force Geophysics Laboratory
Hanscom AFB, Massachusetts 01731
Monitor/M.A.Shea/PH

12. REPORT DATE

11 Oct [redacted] 79

13. NUMBER OF PAGES

28

14. MONITORING AGENCY NAME & ADDRESS (if different from Controlling Office)

9 Final rept.

15. SECURITY CLASS. (of this report)

Unclassified

15a. DECLASSIFICATION/DOWNGRADING SCHEDULE

16. DISTRIBUTION STATEMENT (of this Report)

Approved for public release; distribution unlimited

12 29

DDC
RECEIVED
FEB 8 1980
B

17. DISTRIBUTION STATEMENT (of the abstract entered in Block 20, if different from Report)

15 NOAA [redacted]-01-8-B01-3883

18. SUPPLEMENTARY NOTES

Work performed through National Oceanic and Atmospheric Administration purchase order 01-8-B01-3883

19. KEY WORDS (Continue on reverse side if necessary and identify by block number)

Flares, Flare Prediction, Active Region Velocity Fields

20. ABSTRACT (Continue on reverse side if necessary and identify by block number)

The photospheric line-of-sight velocity field of 24 active regions was examined in relation to the flare activity of the regions. There is a good correlation between the complexity of the velocity field and the level of flare activity in the active region within ±12 hours. Specific velocity patterns could be recognized at 55 of 73 flare sites. Failure to detect patterns

cont'

DD FORM 1473 1 JAN 73 EDITION OF 1 NOV 65 IS OBSOLETE

Unclassified

plus or minus

394 637

Block 20 continued

CONT

at all but one of the remaining flare sites can be understood as due to unfavorable geometry for the detection of the patterns. The specific velocity patterns found at flare sites consist of anomalous Evershed flow patterns in sunspot penumbras (12 of 55 sites), small-scale, mulitpolar velocity structures (15 of 55 sites), and apparent horizontal shears of the velocity field (48 of 55 sites). The shears are frequently but not necessarily associated with magnetic polarity reversal lines. There appears to be a better relation between flare activity and the spatial extent of a velocity shear line than with the strength of the shear. As an aid to predicting the level of flare activity, the velocity complexity of an active region appears to be a practical and valuable parameter. Observations of velocity shears appear to be useful in locating potential flare sites and in estimating the potential size of the flares.

# PHOTOSPHERIC VELOCITY FIELDS AS INDICATORS OF FLARE ACTIVITY

K. Harvey*

Solar Physics Research Corporation

Tucson, Arizona 85718, U.S.A.

and

J. Harvey

Kitt Peak National Observatory**

Tucson, Arizona 85726, U.S.A.

---

* Visiting Astronomer, Kitt Peak National Observatory

**Operated by the Association of Universities for Research in Astronomy, Inc., under contract with the National Science Foundation.

## 1. Introduction

Velocity fields are generally considered to be important in the process of energy buildup leading to flares, but little observational work has been done on this possible relationship. In a previous study of a single active region (Harvey and Harvey, 1976), we found that flares tended to occur where both the velocity and magnetic fields were unusually complex. In particular, flares were found to begin close to locations with inferred strong horizontal velocity shears at the magnetic neutral line. Flare sites and shapes conformed to areas with low line-of-sight velocity surrounded by higher velocities.

In similar but more comprehensive studies, Martres et al. (1971, 1974, 1977) concluded that flares occur at locations where lines separating opposite line-of-sight velocity and magnetic components ($V_{ll} = 0$, $H_{ll} = 0$) cross. They also inferred that a horizontal vortex motion, concurrent with a magnetic field change at or near the $H_{ll} = 0$ line, is a necessary condition for flares to occur.

This study is aimed partly at verifying the conclusions of earlier investigations with superior observations but mainly to address three specific questions: 1. Are there any significant differences in the velocity patterns of active regions with and without flare activity? 2. Do locations of anomalous velocity patterns correlate well with flare locations? 3. Can observations of velocity fields be used to improve predictions of flare activity? We provisionally conclude that the results of previous studies require some modifications and that the answer to all the specific questions is yes.

## 2. Observations

Observations of 24 flaring and non-flaring active regions for periods of 1 to 4 days were made with the 512-channel magnetograph (Livingston et al., 1976) at the 70-cm Vacuum Telescope of the Kitt Peak National Observatory. The observations consisted of digital photoelectric recordings of the intensity, Doppler shift, and longitudinal Zeeman effect of the photospheric 8688 Å FeI line with a spatial element of 1 arc second, a spatial extent of between 512 by 512 arc seconds and 512 by 240 arc seconds, and a time cadence of from 75 to 150 seconds.

As usual, the observed Doppler shift is interpreted as representing the average line-of-sight velocity field in a resolution element although we recognize that line profile variations and line-of-sight integration effects make this simple interpretation somewhat suspect. Similarly, we interpreted the longitudinal Zeeman effect as directly indicating the line-of-sight component of the magnetic field although line-profile variations also complicate this simple interpretation. In our opinion, the errors caused by simple interpretations do not compromise the results of this study.

Although most of the observations were made away from the disc center, the 5-minute photospheric oscillation was still a major source of noise which must be suppressed. Several techniques for suppressing the 5-minute oscillation were tried.

The simplest technique was to average observations made 150 seconds apart in time. This method is far from optimum but does reduce the effects of the oscillation to a considerably smaller level. The technique finally developed consists of taking observations at approximately 75 second intervals and producing weighted averages of groups of 8 such observations. The weights are chosen to approximate a sinc function in time such that the response to temporal variations is essentially zero for variations with periods less than about 6 minutes. This technique removes virtually all traces of the 5-minute oscillation. The magnetic and intensity data were also processed by the same averaging techniques to preserve comparability with the velocity data. The averaging process generally reduced spatial resolution to several arc seconds although seeing was good enough in a few cases to preserve 2 arc second resolution.

Pertinent observational information is collected in Table I. We have included both the McMath and Boulder region numbers and note that many of the McMath regions are identified by Boulder as complexes of two or more regions.

A preliminary list of flares associated with each active region was compiled from reports to the NOAA Space Environment Laboratory and from the weekly NOAA Preliminary Report of Solar Geophysical Data. This list was augmented by examination of Hα patrol films generously lent by NOAA, Boulder, and the Big Bear Solar Observatory. For three of the regions, high-resolution Hα films were lent by Big Bear Solar Observatory and San Fernando Observatory. When possible, published data were compared with the films and found to be generally consistent which gives us confidence in the quality of the published data. A major defect in this study is the inadequate flare patrol coverage available and the resulting uncertainty about exact levels of flare activity and flare locations. Nevertheless, the results should be significant in relative and statistical senses. No efforts were made to correct for incomplete flare data.

## 3. Results

### 3.1 Velocity Complexity and Flare Activity

As shown in Table I, we arbitrarily selected time intervals of 24 hours centered on each series of velocity observations to establish flare activity. Within these time intervals a total of 232 flares, from subflare class to importance 4B, occurred at 73 sites in 18 of the 24 active regions.

Classification of the velocity field is a more subjective procedure which requires elaboration. The simplest velocity patterns we observed in active regions (after suppressing the 5-minute oscillation) consisted of only normal Evershed effect in the sunspot penumbras (if sunspots were present); otherwise the active region was indistinguishable from the quiet sun. Next in complexity is an active region which shows normal Evershed velocities in penumbras and additional structure outside sunspots, but the additional structure is significantly weaker in magnitude than the Evershed velocities. The most complex regions show abnormal Evershed velocities in sunspots and velocities outside sunspots which can rival or exceed the Evershed velocity magnitude. This classification is illustrated in Figure 1.

We can now address the first question posed earlier, and we conclude that there is a significant difference between the photospheric velocity fields of flaring and non-flaring regions. The basis for this conclusion is condensed in Table II. The conclusion holds not only for the entire sample of 24 active regions but also for individual active regions as they evolve.

### 3.2 Velocity Patterns at Flare Sites

A more detailed comparison of the velocity pattern at flare sites is complicated by the fact that we can observe only one component of a three-dimensional velocity vector pattern. To some extent this problem can be resolved by comparing observations at various distances from disc center. With few exceptions we find no correlation between flare sites and velocity patterns when a region is observed near disc center ($\theta < 20°$). Very close to the limb ($\theta > 70°$), foreshortening so degrades the effective spatial resolution that velocity patterns are hard to resolve. Specific velocity patterns have been identified at 55 of the total of 73 flare sites with the best correlation observed at disc center distance $\theta > 30°$. This confirms our earlier result (Harvey and Harvey, 1976) that specific flare activity is related to at least one component of the horizontal velocity field.

We discern three types of velocity patterns at flare locations which are now discussed in detail.

### 3.2.1 Anomalies in Sunspot Evershed Velocity

The normal Evershed velocity pattern of a sunspot penumbra appears as a blue-shifted, non-uniform velocity on the disc-center side of a spot and a red-shifted velocity on the limbward side. Departures from this pattern were observed at 12 flare sites. The types of anomalies observed are: (i) An oppositely-directed velocity structure (5-10 arc seconds in size) imbedded in the otherwise normal surrounding velocity pattern (2 cases). (ii) Absence of a normal Evershed velocity pattern in association with smaller, rapidly growing spots (7 cases). (iii) A strong Evershed velocity pattern on one side of the spot (flare-site) but a much weaker or non-existent pattern on the other side of the spot (3 cases). Such spots were often rapidly developing or showed large proper motions. Figure 2 shows examples of these anomalies.

### 3.2.2 Small-Scale Velocity Structures

At 15 of the 55 velocity-associated flare sites, the velocity pattern consisted of at least two, adjacent, oppositely-directed velocity elements of 3 to 10 arc seconds size. This multipolar velocity structure is observed both in areas without spots and in areas with smaller, rapidly-changing or growing spots. The magnetic field associated with these structures was not necessarily complex and was often unipolar.

### 3.2.3 Shears

The predominant velocity pattern found at flare sites is a velocity shear. We define this as oppositely-directed velocity features in close proximity with an extent in at least one dimension in excess of 10 arc seconds. To detect velocity shears we computed the derivative of the velocity observation in a direction parallel to the limb. This technique largely suppresses the normal Evershed velocity pattern in sunspots but unfortunately only reveals one component of a (presumably) two-dimensional, horizontal shear pattern.

Velocity shears were identified at 48 of the 55 velocity-associated flare sites. There appears to be a much better correlation between the spatial extent of a velocity shear and the associated level of flare activity (Table III) than between the strength of a shear and associated flare activity. An example of a long shear line is shown in Figure 3. In most cases the velocity shear is closely related to the $H_{11} = 0$ line (see below) but in 19 of the 48 shear examples there is no such association. In these cases the shears appear to be the result of (i) the combined Evershed velocity pattern of several sunspots in close proximity or multiple umbrae within a single penumbra, (ii) anomalous small-scale velocity structure within the normal Evershed pattern or, (iii) multipolar velocity structures located in an area of unipolar magnetic flux.

### 3.2.4 Flares without Velocity Pattern

For 18 of the 73 flare sites studied, no identifiable velocity pattern could be found. Geometric considerations explain most of this lack of correlation. Ten of the flare sites were located in regions within 20° of the disc center. If the velocity field associated with flares is horizontal, the poor sensitivity to such fields near disc center explains these cases. The remaining 8 flare sites were in 5 regions observed away from disc center ($\theta > 30°$). In 4 regions the $H_{11} = 0$ line was parallel to the limb and if a velocity shear was present and parallel to the $H_{11} = 0$ line, as is usually the case, we would be unable to detect it in these cases. The one remaining flare site was located between two active regions and the lack of an associated velocity pattern cannot currently be explained.

### 3.3 Association of Velocity and Magnetic Patterns

We examined the magnetic pattern at the 48 flare sites which were associated with velocity shears. It was generally possible to construct $H_{11} = 0$ lines as well as $V_{11} = 0$ and shear lines. In 29 of the 48 cases an $H_{11} = 0$ line was located near the flare site ( and $V_{11} = 0$ and velocity shear line). In some of these cases, the $H_{11} = 0$ and $V_{11} = 0$ lines crossed in agreement with the results of Martres <u>et al</u>. (1971, 1974, 1977). However, in most of the 29 cases, the velocity shear, $V_{11} = 0$, and $H_{11} = 0$ lines were roughly parallel. There was frequently a 3 to 8 arc second displacement of the $H_{11} = 0$ line. Thus the requirement of Martres <u>et al</u>. is not confirmed for all of the events in our sample.

In the 7 cases of distinctive velocity patterns at flare sites without shear patterns, the magnetic field was either unipolar and undistinguished or so complicated by small-scale structure as to defy construction of $H_{11} = 0$ lines.

In Figure 4 we treated the magnetic pattern the same way as the velocity pattern to obtain a magnetic "shear" pattern. This illustrates the similarity between the $H_{11} = 0$, $V_{11} = 0$, and shear lines. It also shows a complexity of the magnetic "shear" picture which is greater than in the velocity shear picture with several features unrelated to flare activity.

### 3.4 Time Changes in the Velocity Field and Flare Association

Long time series of observations suitable for a study of velocity variations in association with flares were not generally taken during this study. For one region (Boulder 1203), a time sequence was available for a few hours on each of three days. On one of the days, changes in the velocity pattern were observed which suggested an association with subsequent flares. In one case, a blue-shifted velocity element appeared 90 minutes prior to the onset of a flare, and in the second case, an existing blue-shifted feature strengthened 100 minutes prior to a flare. In both areas flare activity was observed only after the onset of the velocity change. No corresponding magnetic or intensity changes were noted. This is hardly compelling evidence but is consistent with preflare blue shifts reported by Harvey and Harvey (1976) and others on previous occasions.

### 3.5 Velocity Fields as an Aid to Predicting Flares

The velocity field pattern is not a perfect guide to predicting flare activity, size, or location. A suitably blind test was not conducted during this study, but some results look promising for further investigation. On the positive side, there is a very good correlation between flare activity and velocity complexity.

Anomalies of the Evershed pattern, if associated with shears of the velocity pattern, were invariably the site of flare activity within ±12 hours. Large-scale velocity shears were associated with flare sites in every case. Evidence that a photospheric blue shift precedes flares was strengthened. Velocity shear patterns are relatively easier to interpret than magnetic field patterns.

On the negative side, no significant velocity pattern was found at nearly 1/4 of the flare sites studied. The fact that this can be explained as due to geometry does not make the failure any smaller. Velocity shears were identified at 8 locations at which no flares were reported. These shears were weak and small in extent and possibly unreported flares did occur at the sites, but, based on available data, these shears represent a failure of the shear pattern as a flare-site predictor. We suspect that photospheric blue-shifted features appear and disappear all the time, and some additional criterion is required if such features are to be useful as flare precursors.

Fourier transforms of the velocity pattern of several of the active regions were computed in the hope that some distinctive signature of a flare-rich active region could be found. The transforms were dominated by the Evershed effect and the spacing of sunspots in the active regions and yielded nothing in the way of a clear signature representing flare activity. We believe that the shear pattern is much more useful, and it is certainly easier to compute. It is possible that some simple parameter of a shear map such as RMS shear could be an effective single parameter to characterize the flare potential of an active region, but a more extensive investigation is required.

## 4. Conclusions

We conclude from this limited study that the complexity of the photospheric velocity field is closely associated with the level of flare activity in an active region. Further, the sites of flare activity are closely associated with specific velocity patterns, expecially apparent horizontal velocity shears. The spatial extent of such shears appears to be related to the magnitude of flare activity. Finally, although geometric problems are a limiting factor, observations of the velocity field are practical and can provide valuable additional information to help predict the flare potential of active regions.

## Acknowledgments

This study was support in part by the Air Force Geophysics Laboratory project order ESD 8-0927 through NOAA ~~Purchase~~ Order 01-8-B01-3883.

We are grateful to G. Heckman of the Space Environment Laboratory of NOAA for his personal interest in supporting this study and to F. Recely of NOAA for making many of the observations and to B. Gillespie for taking most of the remaining observations. The operation of the Vacuum Telescope at Kitt Peak National Observatory is partially supported by NOAA. Flare and Hα film data were kindly provded by M. Pierce and M. Losleben of the Space Environment Laboratory, F. Tang and H. Zirin of Big Bear Solar Observatory, and S. Martin of San Fernando Observatory.

## References

Harvey, K. L. and Harvey, J. W.: 1976, "A Study of the Magnetic and Velocity Fields in an Active Region," Solar Phys. 47, 233.

Livingston, W. C., Harvey, J, Slaughter, C, and Trumbo, D.: 1976, "Solar Magnetograph Employing Integrated Diode Arrays," Appl. Opt. 15, 40.

Martres, M. -J., Soru-Escaut, I. and Rayrole, J.: 1971 in R. Howard (ed.) "An Attempt to Associate Observed Photospheric Motions with the Magnetic Field Sturcture and Flare Occurrence in an Active Region," Solar Magnetic Fields, IAU Symposium 43, p. 435.

Martres, M. -J., Rayrole, J., Ribes, E., Semel, M., and Soru-Escaut, I.: 1974, " On the Importance of Photospheric Velocities in Relation to Flares," in Flare-Related Magnetic Field Dynamics Conference, Boulder, Colorado, p. 333.

Martres, M. -J. and Soru-Escaut, I.: 1977, "The Relation of Flares to 'Newly Emerging Flux' and 'Evolving Magnetic Features'," Solar Phys. 53, 225.

TABLE I

Ledger of Observations

| Region McMath | Region Boulder | Date Observed (1978) | Time Observed (UT) | Region Position | Mag Class[1] | Vel Class[2] | Flaring Level | Number of Flares ±12 Hrs | Number of Flares ±3 Hrs | Number of Flares Major ≥ IMP 2 |
|---|---|---|---|---|---|---|---|---|---|---|
| 15266 | 1092 | 4-28 | 2319-22 | N25E37 | δ+βp | C | High | 11 | 4 | 4B 1308[+] |
| 15403 | 1203 | 7-11 | 1734-1821 | N18E41 | δ | C | High | 20 | 8* | 2B 1049 & 2215 |
| | | 7-13 | 1549-1846 | E16 | δ | C | Moderate | 23 | 14* | |
| | | 7-14 | 1808-2103 | E03 | δ | C | Moderate | 23 | 13* | |
| 15525 | 1284 | 9-7 | 1704-07 | N33E55 | β | A | Moderate | 9 | 5 | |
| | | 9-8 | 1604-07 | E46 | β | A | Low | 4 | 3 | |
| | | 9-9 | 1740-43 | E34 | β | Q | Quiet | 1 | 1 | |
| | | 9-10 | 1548-51 | E25 | β | Q | Low | 3 | 0 | |
| 15509 | 1272 | 9-7 | 1713-16 | S32W28 | β | A | Low | 10 | 3 | |
| | | 9-8 | 1620-23 | W42 | β | A | Low | 7 | 5* | |
| | | 9-9 | 1749-51 | W55 | β | A | Moderate | 10 | 3 | |
| | | 9-10 | 1554-57 | W65 | β | Q | Low | 2 | 2 | |
| 15526 | 1282 | 9-7 | 1713-16 | S23W32 | β | A | Low | 11 | 6 | |
| | | 9-8 | 1620-23 | W44 | β | A | Moderate | 7 | 5* | |
| | | 9-9 | 1749-51 | W56 | β | Q | Quiet | 1 | 0 | |
| | | 9-10 | 1554-57 | W69 | β | A | Low | 3 | 3* | |
| 15543 | 1294 | 9-21 | 1901-16 | N36W29 | βγ | A | Moderate | 16 | 9* | |
| | | 9-22 | 1754-1809 | W43 | βγ | A | Low | 5 | 3* | |
| | | 9-23 | 1613-28 | W53 | β | A | High | 9 | 0 | 3B 0947[+] |
| 15536 | 1289 | 9-21 | 1901-16 | N28W38 | αp | Q | Quiet | 0 | 0 | |
| | | 9-22 | 1754-1809 | W58 | αp | Q | Quiet | 3 | 0 | |
| | | 9-23 | 1613-28 | W67 | αp | Q | Quiet | 2 | 0 | |
| 15532 | 1287 | 9-21 | 1901-16 | N37W43 | αp | Q | Quiet | 0 | 0 | |

| Region | | Date | Time | Region | Mag | Vel | Flaring | Number of Flares | | |
|---|---|---|---|---|---|---|---|---|---|---|
| McMath | Boulder | Observed (1978) | Observed (UT) | Position | Class[1] | Class[2] | Level | ±12 Hrs | ±3 Hrs | Major ≥ IMP 2 |
| | | 9-22 | 1754-1809 | W59 | αp | Q | Low | 2 | 2 | |
| | | 9-23 | 1613-28 | W72 | αp | Q | Quiet | 0 | 0 | |
| 15598 | 1351 | 10-17 | 1538-49 | N31E40 | β | A | Low | 3 | 1 | |
| | | 10-18 | 1637-48 | E24 | βγ | A | Low | 2 | 0 | |
| 15597 | 1350 | 10-17 | 1538-49 | N20E32 | αp | Q | Low | 2 | 0 | |
| | | 10-18 | 1637-48 | E17 | αp | Q | Quiet | 0 | 0 | |
| 15591 | 1348 | 10-17 | 1551-1601 | S22W10 | β | Q | Quiet | 1 | 0 | |
| | | 10-18 | 1650-1700 | W23 | β | Q | Low | 5 | 0 | |
| 15587 | 1346 | 10-17 | 1605-17 | S20W50 | β | A | Low | 7 | 4 | |
| | | 10-18 | 1703-13 | W65 | β | Q | Quiet | 0 | 0 | |
| | 1344 | 10-17 | 1605-17 | S24W52 | α | Q | Quiet | 0 | 0 | |
| | | 10-18 | 1703-13 | W67 | - | Q | Quiet | 0 | 0 | |
| | 1335 | 10-17 | 1605-17 | S20W62 | αp | Q | Quiet | 1 | 0 | |
| | | 10-18 | 1703-13 | W77 | αp | Q | Quiet | 0 | 0 | |
| 15587 | 1352 | 10-17 | 1605-17 | S21W57 | - | Q | Quiet | 0 | 0 | |
| | | 10-18 | 1703-13 | W73 | - | Q | Quiet | 0 | 0 | |
| 15586 | 1336 | 10-17 | 1605-17 | S31W62 | - | Q | Quiet | 0 | 0 | |
| | | 10-18 | 1703-13 | W75 | - | Q | Quiet | 0 | 0 | |
| 15631 | 1371 | 10-26 | 1834-1921 | S13E81 | β | Q | Quiet | 0 | 0 | |
| | | 10-27 | 1734-43 | E65 | αp | Q | Quiet | 0 | 0 | |
| | | 10-28 | 1531-40 | E54 | αp | Q | Quiet | 0 | 0 | |
| 15619 | 1365 | 10-28 | 1745-1852 | N20E05 | βγ | Q | Moderate | 4 | 1 | 2B 1557 |
| | 1370 | 10-28 | 1745-1852 | N24W01 | β | Q | Low | 0 | 0 | |
| 15620 | 1366 | 10-28 | 1907-16 | S19E13 | αp | Q | Low | 1 | 0 | |
| 15621 | 1367 | 10-28 | 1907-16 | S24E03 | - | Q | Low | 1 | 1 | |

| Region | | Date | Time | Region | Mag | Vel | Flaring | Number of Flares | | |
|---|---|---|---|---|---|---|---|---|---|---|
| McMath | Boulder | Observed (1978) | Observed (UT) | Position | Class[1] | Class[2] | Level | ±12 Hrs | ±3 Hrs | Major $\geq$ IMP 2 |
| 15641 | 1382 | 11-4 | 2039-2108 | S11E38 | β | A | Low | 8 | 4 | |
| | | 11-5 | 1957-2006 | E25 | βγ | A | Low | 7 | 5* | |
| 15642 | 1374 | 11-4 | 2116-34 | S26E01 | β | Q | Quiet | 2 | 1 | |
| | | 11-5 | 2009-35 | W11 | β | Q | Quiet | 2 | 0 | |
| | 1381 | 11-4 | 2116-34 | S18W10 | β | Q | Quiet | 0 | 0 | |
| | | 11-5 | 2009-35 | W24 | β | Q | Low | 4 | 2 | |

1. Mt. Wilson Magnetic Classification.

2. C = complex, A = active, Q = quiet
   See Section 3.1 for definition of Velocity Complexity.

*Flare or Flares occurred during velocity observations.

+Proton Flare

Flaring Level
- High: 1-3 IMP $\geq$ 2 flares per day with M/X level X-rays.
- Moderate: 7-15 flares per day with $\geq$ 1 IMP 1 flare, C/M level X-rays.
- Low: 1-8 subflares per day, C level X-rays.
- Quiet: $\leq$ 1 subflare per day, no X-ray events.

TABLE II

Distribution of 54 determinations of velocity complexity and flare activity within ±12 hours.

| Velocity Complexity | Flare Level: Quiet | Low | Moderate | High |
|---|---|---|---|---|
| Complex | 0 | 0 | 2 | 2 |
| Active | 0 | 11 | 4 | 1 |
| Quiet | 24 | 9 | 1 | 0 |

## TABLE III

Flare activity related to length of velocity shear (corrected for foreshortening)

| Number of Flares (±12 hrs.) | Length of shear (arc seconds) | | | | | |
|---|---|---|---|---|---|---|
| | $\leq 5$ | 5-10 | 10-15 | 15-25 | 25-45 | > 45 |
| IMP $\geq 2$ (all classes) | 0 | 1 | 0 | 0 | 0 | 3 |
| > 10 | 0 | 0 | 0 | 0 | 1 | 1 |
| 6-10 | 0 | 1 | 1 | 0 | 1 | 0 |
| 3-6 | 0 | 4 | 7 | 3 | 0 | 2 |
| 2-3 | 1 | 8 | 4 | 1 | 0 | 0 |
| $\leq 1$ | 7 | 9 | 3 | 2 | 0 | 0 |

## Figure Captions

Fig. 1. Examples of velocity field complexity classification. (top) Velocity field with black representing approach and white recession. (bottom) Intensity images in exact register with the velocity images. The extent of the observations is 207 arc seconds east-west by 256 arc seconds north-south. North is to the left and east to the top. (a) A quiet velocity pattern (Boulder region 1371 on October 28, 1978). (b) An active velocity pattern (Boulder region 1382 on November 4, 1978). (c) A complex velocity pattern (Boulder region 1203 on July 11, 1978).

Fig. 2. Examples of Evershed velocity anomalies at flare sites. (top) Velocity field with black representing approach and white recession. (bottom) Intensity images in exact register with the velocity images. The extent of the observations is 64 by 64 arc seconds. North is to the left and east to the top. (a) The arrow indicates a dark velocity feature in the Evershed pattern where a light feature is expected (Boulder region 1203 on July 14, 1978). (b) The arrow indicates a spot with no Evershed velocity pattern; instead, a completely anomalous pattern is seen (Boulder region 1203 on July 11, 1978). c) The arrow indicates a sunspot with no Evershed velocity on one side (Boulder region 1351 on October 18, 1978).

Fig. 3. Boulder region 1092 on April 28, 1978. Each frame covers an area of 256 by 256 arc seconds with north to the left and east to the top. (top left) Velocity image with black representing approach and white recession. (top right) Velocity shear

image with x's indicating flare sites. (bottom left) Magnetic field with white representing a field toward the observer and black away from the observer. (bottom right) Intensity image.

Fig. 4. Boulder region 1203 on July 13, 1978. Each frame covers an area of 256 by 256 arc seconds with north to the left and east to the top. (top left) Velocity image with black representing approach and white recession. (top right) Velocity shear image with x's indicating flare sites. (bottom left) Magnetic field with white representing a field toward the observer and black away from the observer. (bottom right) A magnetic field "shear" image produced in the same way as the velocity shear image but from the magnetic data rather than the velocity data. Strong features are present which have no relation to flare activity.

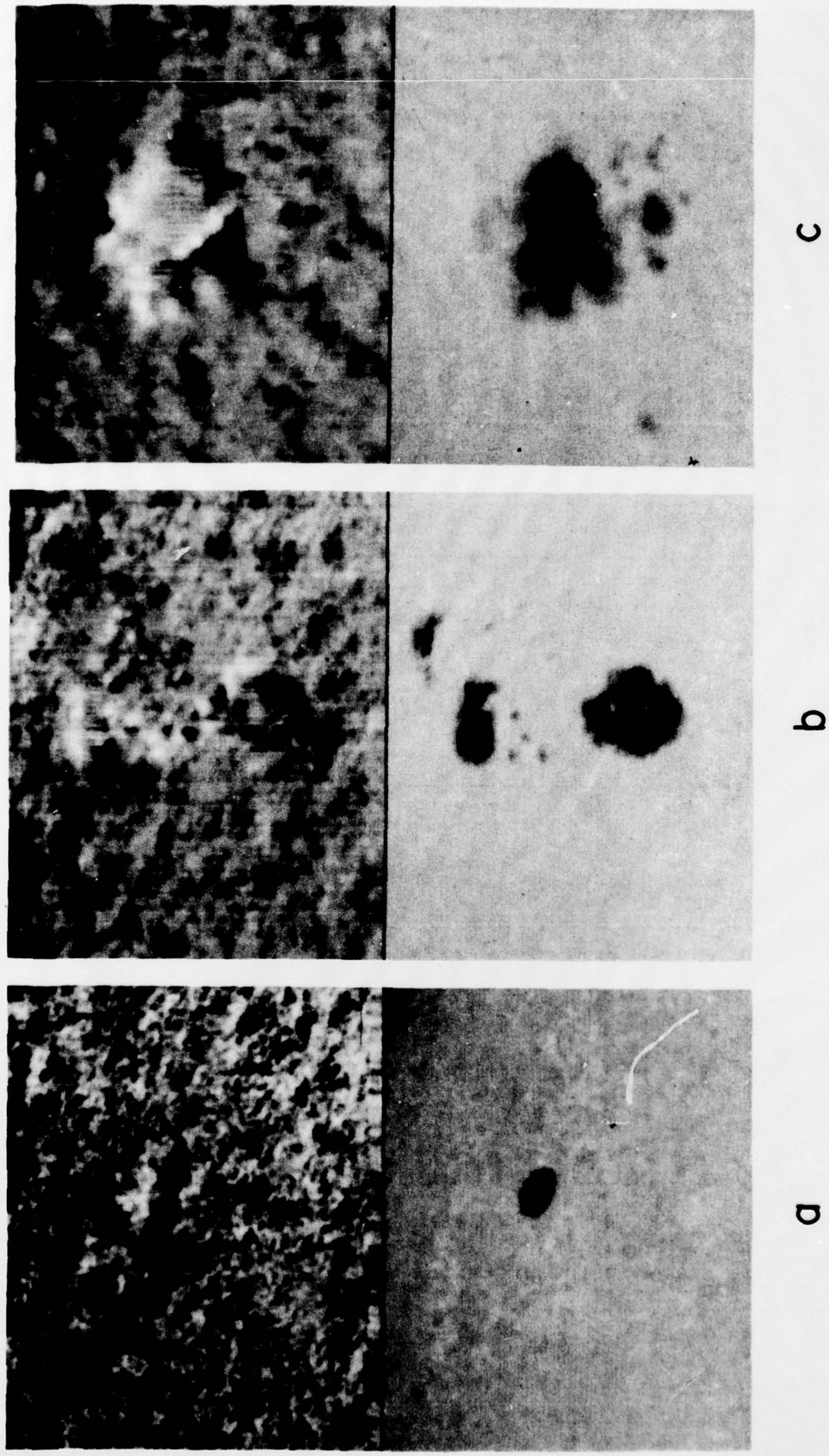


Figure 1

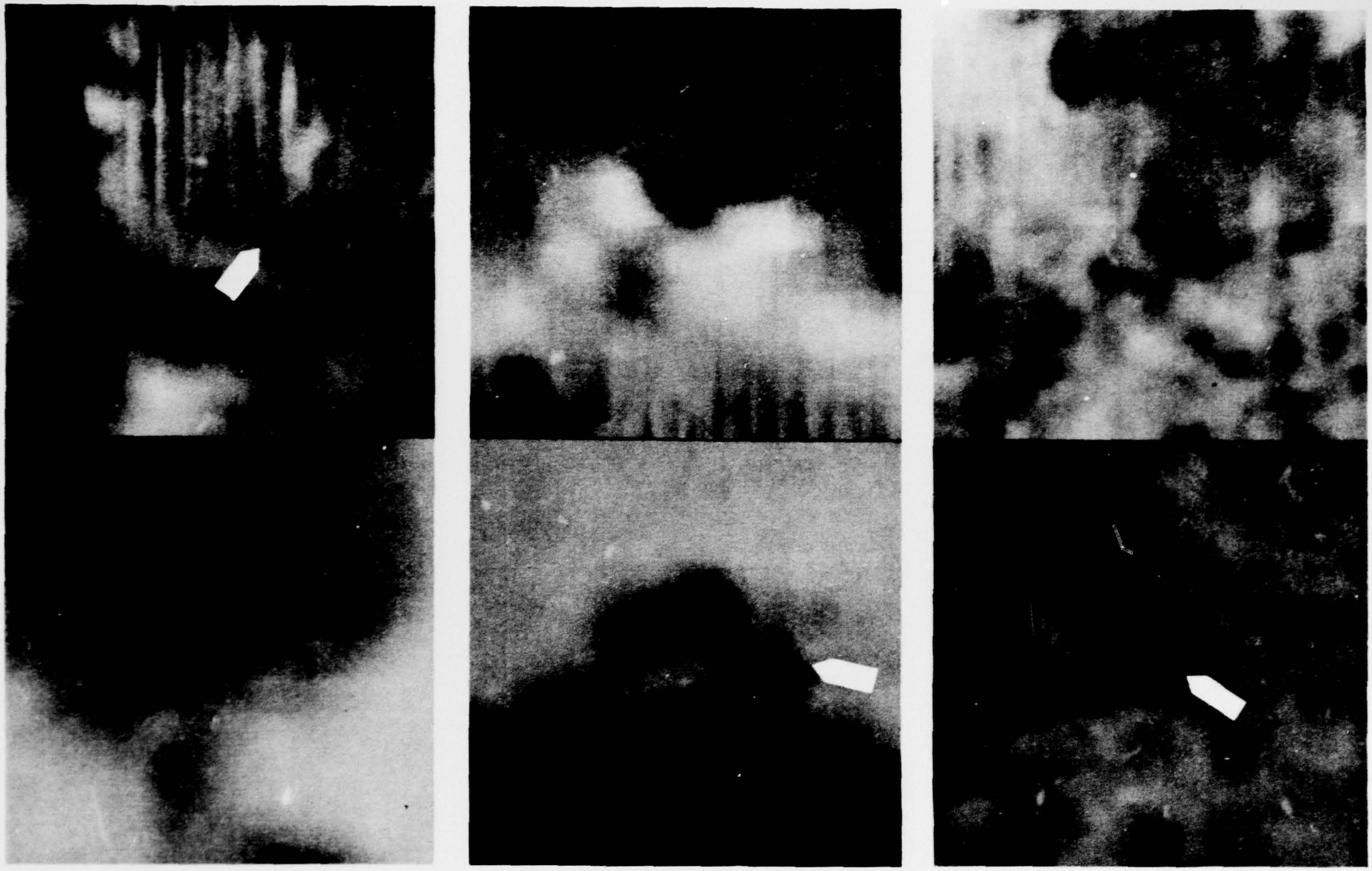


Figure 2

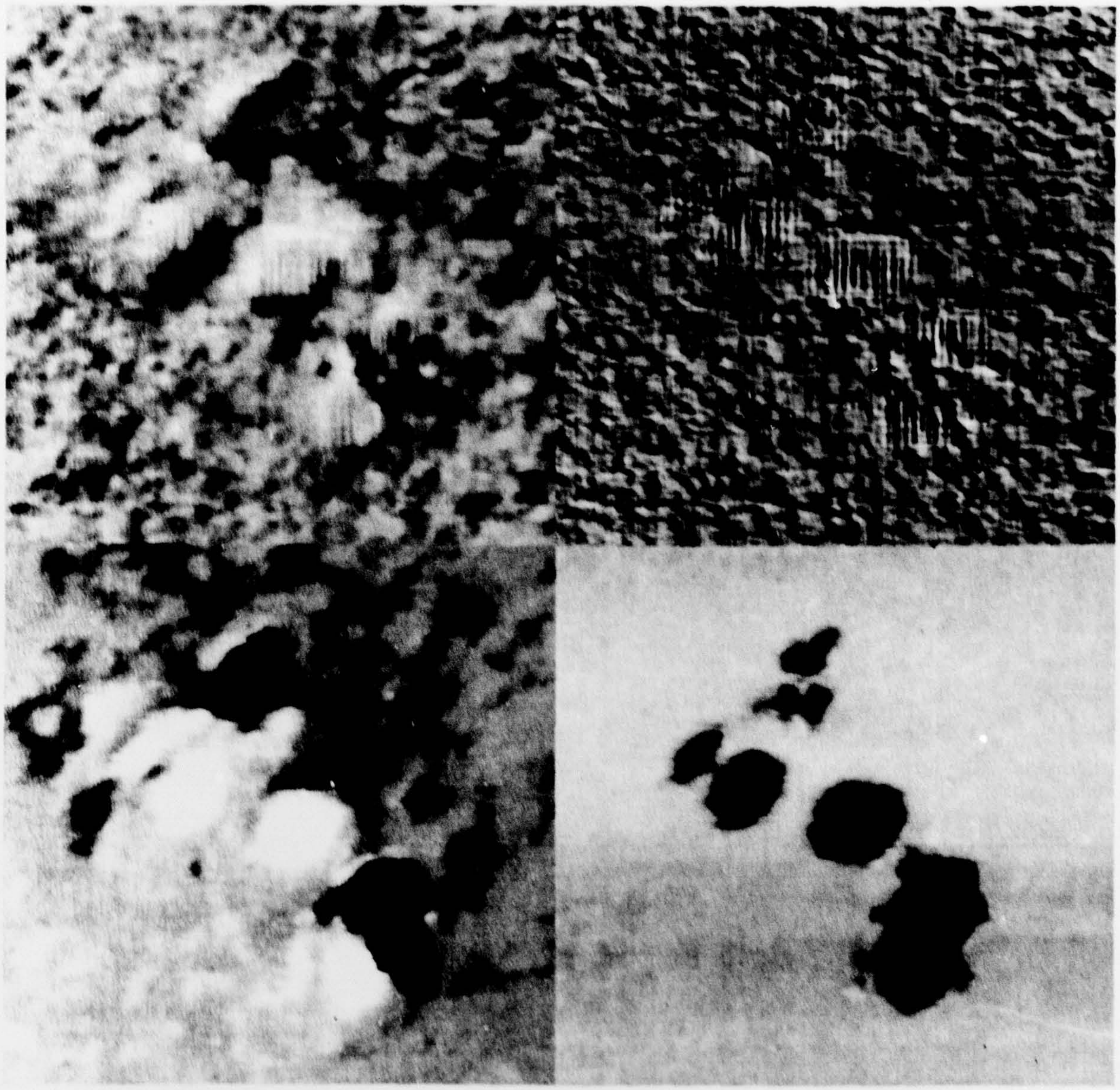

Figure 3

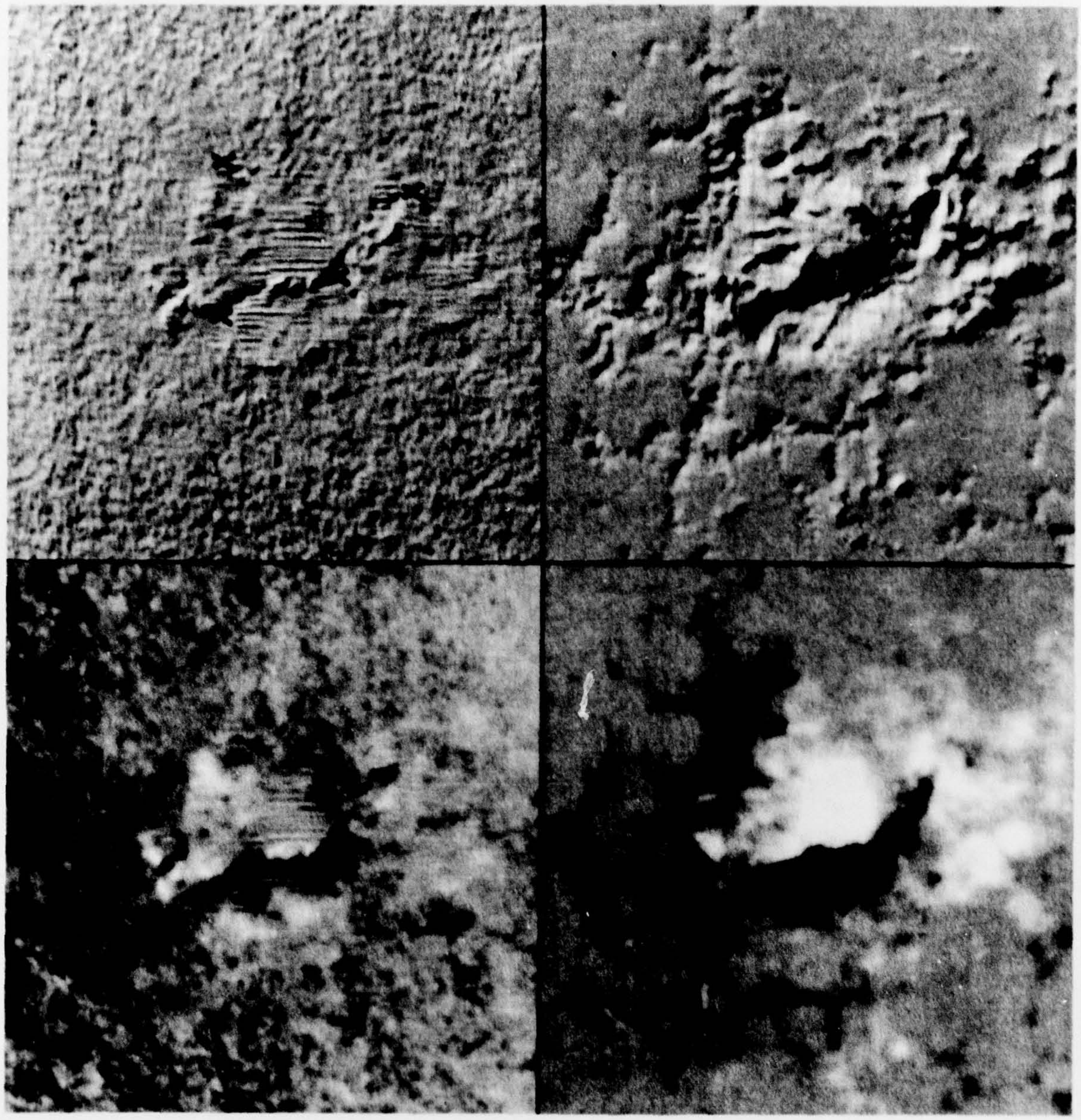

Figure 4